

# SINGLE PULSE DAMAGE IN COPPER

M. C. Ross, R. Iverson, K. Jobe, D. McCormick, P. Tenenbaum, P. Raimondi, SLAC, Stanford, CA94309, USA\*

## Abstract

The Next Linear Collider (NLC)[1] electron and positron beams are capable of damaging the linac accelerating structure and beamline vacuum chambers during a single accelerator pulse. Machine protection system (MPS) considerations have an impact on the engineering and design of most machine components downstream of the damping ring injector complex. Beam tests have been done at the SLAC Final Focus Test Beam (FFTB)[2] to examine the behavior of copper at and above the damage stress threshold. In this paper we present results of damage studies in copper as the beam pulse heating is varied from below melting to near vaporization. The goal of the tests was to determine allowable limits on beam size and intensity of a benign single bunch pilot beam to be used in testing linac systems. Typical expected pilot beam parameters (compared with nominal) are: 10 times reduced intensity, 10 times increased horizontal emittance and 1000 times increased vertical emittance, resulting in a reduction in charge density of  $10^5$ . The tests we report here used short (1 mm) beam pulses of between  $I = 3 \times 10^9$  and  $20 \times 10^9$  electrons with transverse sizes  $\sigma_{xy}$  between  $45 \mu\text{m}^2$  and  $200 \mu\text{m}^2$ .

## 1 INTRODUCTION

The design requirements for the NLC MPS are summarized in reference [3]. The geometry of the linear collider makes it impossible to abort an errant pulse once it has been launched into the main 10 km X-band linac. Since there is no guarantee that the first pulse will traverse the system properly, the pilot must be harmless. The purpose of the single pulse damage test was to determine the pilot pulse parameters. Energy deposition simulations indicated that the pilot pulse should have both a large emittance and a small intensity, forcing beam instrumentation to have an extended dynamic range.

It is critical to understand what constitutes damage in the X-band linac structure. It is possible that the structure performance will be degraded by impact from relatively low intensity ( $<0.01$  of  $I$  nominal) pulses. In this series of tests, we hope to examine the change in the crystalline structure of the copper surrounding the impact point. Here, however, we only present images showing significant surface damage. NLC X-band structure high

power tests[4] will indicate limits on structure crystalline and surface damage.

There are three thermal thresholds of interest, as illustrated in table 1. The bottom line of the table shows the temperature at which annealed copper will mechanically yield, i.e. the stresses from the beam heating exceed the tensile elastic limit. [5]

Table 1: Properties of Copper.

|                | E_dep (J/gm) | Temp. (°C) |
|----------------|--------------|------------|
| Vaporization   | 4800         | 2570       |
| Melting        | 400          | 1083       |
| Local yielding | 62           | 180        |

Downstream of the linac, damage concerns are limited to simple vacuum chambers, collimation systems and special instruments. The latter will be protected through local optics and design. The series of single pulse damage tests will allow us to determine the threshold beam parameters which generate loss of vacuum integrity.

## 2 DAMAGE ESTIMATES

We used a coupon 1.4 mm thick, the same thickness as the iris of the X-band disk loaded waveguide structure. The interaction between the beam and the material was modelled using the EGS code, originally developed for use with electromagnetic showers. Table 2 shows the calculated energy deposition and resultant temperature rise in the material for beam parameters used in this test and for typical NLC linac beam parameters. Copper boils at 2570 °C; it will be fully vaporized by an energy deposition of  $\sim 4800\text{J/gm}$ .

Table 2: Estimated energy deposition and temperature in the copper test coupon for test beam and typical NLC linac beam parameters.

| #  | $\sqrt{\sigma_x \sigma_y}$ | $I \times 10^{10}$ | E (J/gm) | T (°C) |                         |
|----|----------------------------|--------------------|----------|--------|-------------------------|
| 1  | 7                          | 2                  | 2425     | 2570   | fix $\sigma$ , vary $I$ |
| 2  | 7                          | 1.6                | 1940     | 2570   |                         |
| 3  | 7                          | 1.0                | 1210     | 2570   |                         |
| 4  | 7                          | 0.7                | 850      | 2200   |                         |
| 5  | 7                          | 0.3                | 360      | 920    |                         |
| 6  | 8                          | 2                  | 1615     | 2570   | fix $I$<br>var $\sigma$ |
| 7  | 10                         | 2                  | 1175     | 2570   |                         |
| 8  | 14                         | 2                  | 550      | 1430   |                         |
| 9  | 7                          | 100                | 120000   | -      | typ                     |
| 10 | 4                          | 100                | 360000   | -      | NLC                     |

\* Work supported by U. S. Department of Energy, Contract DE-AC03-76SF00515

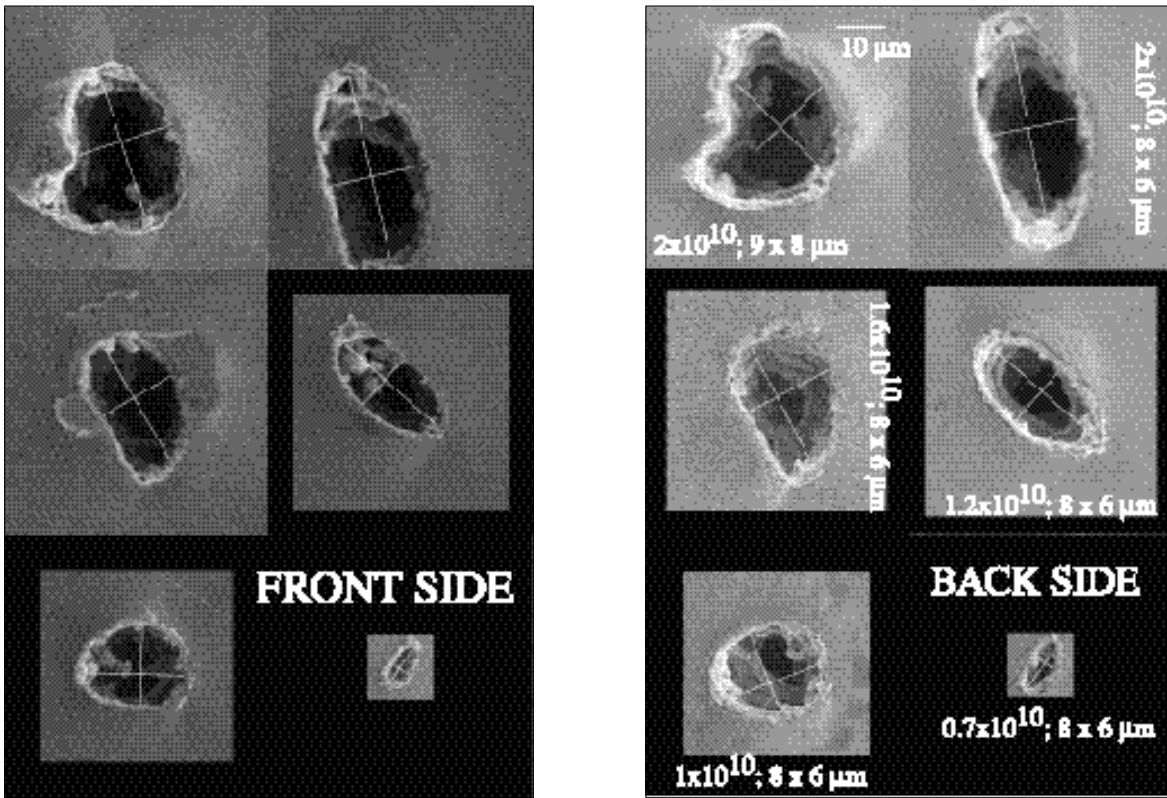


Figure 1: Scanning electron microscope (SEM) images of the entrance (left) and exit (right) points on the copper coupon. The faint lines drawn in the figure were used to estimate the impact point size. All of the images in the montage have the same scale.



Figure 2: Sketch of a section of the copper coupon showing beam impact points (IPs) and associated parameters. The coupon size is 34 x 13 mm.

### 3 DAMAGE TESTS AND ANALYSIS

The beam tests were performed in the SLAC Final Focus Test Beam area, near the focal point in the system, where the beams can be made quite small. We used wire scanner mechanics and controls originally developed for use at the SLAC Linear Collider [6] to position the coupon in the beam path. A magnet near the entrance to the linac was used to allow beam through to the FFTB, one pulse at a time, such that the coupon could be moved 200 μm between pulses. Seven micron wires mounted on the mover to the side of the coupon allow precise positioning of the beam with respect to the coupon and provide local measurements of the beam size.

Figure 1 shows the scanning electron microscope images of selected impact points (IPs), out of a total of 134 image pairs. Both the front and back side of an IP is

shown in the figure, with the images manipulated so that the spot has the same orientation.

Extreme heating followed by rapid cooling is evident from the complex surface of each IP. It also appears that some of the material is missing, leaving a substantial pit whose depth is comparable to its size. This indicates high pressure in the material along the path of the beam, with force enough to eject the liquid at the surface. We are led to conclude that some of the copper was in the gas phase, even though predictions did not indicate enough heat for full vaporization. It is possible that there is additional heat deposition from local electric currents produced by the strong field of the beam ( $I^2R$  heating'), as predicted for collimator surfaces [7]. Subsequent tests using a helium based vacuum system leak detector showed small,  $10^{-8}$  torr/liter/sec, leaks through the coupon in the region of the larger IPs.

Figure 2 shows a diagram of the test coupon with the IPs. There are 12 groups of 10 (or 15) impact points spaced with 2 mm gaps. For each IP, the beam intensity and trajectory parameters were recorded. The correspondence between the IP and the beam pulse was made through examination of the pattern. The high intensity IPs, which make interesting pictures, but are not the focus of the study, allowed easy identification and enabled us to pinpoint the locations of threshold IPs, with either low intensity or large beam sizes.

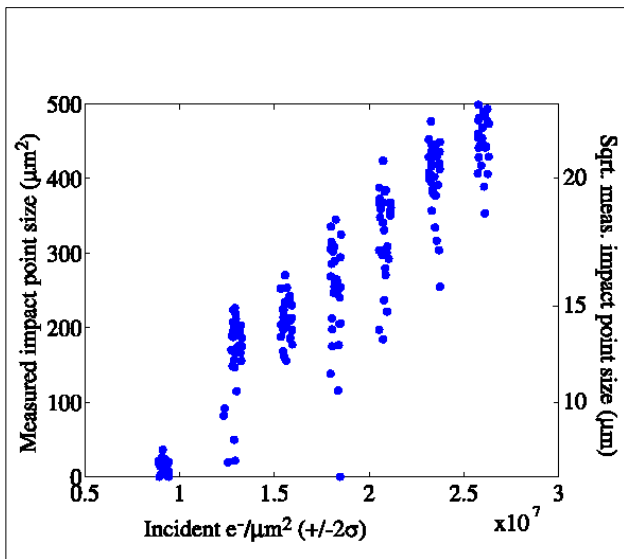


Figure 3: Measured impact point sizes vs beam density.

Two groups of IPs, (rows 5 and 8 in table 2) were clearly visible with a naked eye, but were not found with the low magnification SEM. The estimated temperature rise for these two groups is close to the melting point, but no eruption-like behavior took place. The markings seen by eye may be little more than slightly discolored regions. Since the locations of the IPs can be accurately extrapolated using the surrounding groups, future tests will include localized crystallographic analysis.

Figure 3 shows the measured IP sizes as a function of the incident beam density for the data set where  $\sigma_{xy}$  was fixed ( $8 \times 6 \mu\text{m}$ ) and  $I$  was varied ( $0.7 \times 10^{10} < I < 2 \times 10^{10}$ ). Linear behavior with an apparent threshold near  $10^7 \text{ e}^-/\mu\text{m}^2$  can be seen in the figure. The spot size measurements were made by scaling the images along the major axis of the IP (shown as faint lines in figure 1). The major axes are usually not rotated in the beam  $x$   $y$  coordinate system.

#### 4 CONCLUSIONS

The test validated the technique using the wire scanner and beam control system. The estimated pilot beam parameters, published in [3], assumed a very conservative temperature rise limit of  $180^\circ\text{C}$ , corresponding to a beam density of  $2.2 \times 10^5 \text{ e}^-/\mu\text{m}^2$ , 50 times lower than the lowest density used in this test. We hope to use the

technique to extend our studies of damage to beam densities both below and above those reported here.

Future experiments will test materials to be used in vacuum, positron production target and collimation systems. This includes stainless steel, aluminum, tungsten (and tungsten/rhenium) and special collimator materials such as graphite. Additionally, we hope that the studies will be of use for materials research in general.

#### ACKNOWLEDGEMENTS

We would like to acknowledge the effort of J. McKee and S. McKee who manually analyzed the SEM images. We also acknowledge the microscope operators of the SLAC Physical Electronics Department and note that we had valuable discussions with John Cornuelle, Earl Hoyt and Josef Frisch.

#### REFERENCES

- [1] T. Raubenheimer, "Progress in the Next Linear Collider Design", Linac 2000, Monterey, August 2000.
- [2] V. Alexandrov, et.al., "Results of Final Focus Test Beam", PAC95, Dallas, May 1995.
- [3] C. Adolphsen, et.al., "The Next Linear Collider Machine Protection System", PAC99, New York, March 1999
- [4] C. Adolphsen, "RF Processing of X-band Structures at the NLCTA", LINAC2000, Monterey, August 2000.
- [5] "Next Linear Collider Zeroth Order Design Report", pp 889 - 905, SLAC 1996.
- [6] M. Ross, "Wire Scanner Systems for Beam Size and Emittance Measurements at SLC", Beam Instrumentation Workshop Proceedings (AIP Conference Proceedings 229), Batavia, 1990.
- [7] J. Frisch, et.al., "Advanced Collimator Systems for the NLC", LINAC2000, Monterey, August 2000.